

# Crystal structure of squid rhodopsin

Midori Murakami<sup>1</sup> & Tsutomu Kouyama<sup>1,2</sup>

Invertebrate phototransduction uses an inositol-1,4,5-trisphosphate signalling cascade in which photoactivated rhodopsin stimulates a G<sub>q</sub>-type G protein, that is, a class of G protein that stimulates membrane-bound phospholipase C $\beta$ . The same cascade is used by many G-protein-coupled receptors, indicating that invertebrate rhodopsin is a prototypical member. Here we report the crystal structure of squid (*Todarodes pacificus*) rhodopsin at 2.5 Å resolution. Among seven transmembrane  $\alpha$ -helices, helices V and VI extend into the cytoplasmic medium and, together with two cytoplasmic helices, they form a rigid protrusion from the membrane surface. This peculiar structure, which is not seen in bovine rhodopsin, seems to be crucial for the recognition of G<sub>q</sub>-type G proteins. The retinal Schiff base forms a hydrogen bond to Asn 87 or Tyr 111; it is far from the putative counterion Glu 180. In the crystal, a tight association is formed between the amino-terminal polypeptides of neighbouring monomers; this intermembrane dimerization may be responsible for the organization of hexagonally packed microvillar membranes in the photoreceptor rhabdom.

G-protein-coupled receptors (GPCRs) are activated by a variety of external physical and chemical stimuli and they transmit the stimuli to intracellular signalling cascades by activation of G proteins at the cytoplasmic surface<sup>1</sup>. Rhodopsin is the primary photoreceptor molecule in the visual signalling cascade<sup>2–4</sup>. Like other visual pigments, invertebrate rhodopsin contains 11-*cis* retinal attached to a lysine residue, the photoisomerization of which results in the activation of a heterotrimeric G protein (guanine-nucleotide-binding protein). In contrast to vertebrate vision, in which signal transduction is mediated by the second messenger cyclic GMP, invertebrate phototransduction uses an inositol-1,4,5-trisphosphate signalling cascade in which a

G<sub>q</sub>-type G protein is stimulated by photoactivated rhodopsin<sup>5</sup>. As the latter is used by numerous GPCRs, invertebrate rhodopsin can be regarded as a prototypical member of the GPCR family.

## Crystal structure of squid rhodopsin

Squid (*Todarodes pacificus*) rhodopsin contains 448 amino acids with a molecular mass of ~50 kDa<sup>6</sup>. Its polypeptide chain is ~100 residues longer than those of vertebrate counterparts, primarily due to a 10-kDa carboxy-terminal extension containing proline-rich sequences (Fig. 1). This C-terminal extension is important in the regulation of intracellular trafficking and photoreceptor morphogenesis<sup>7</sup>, but its

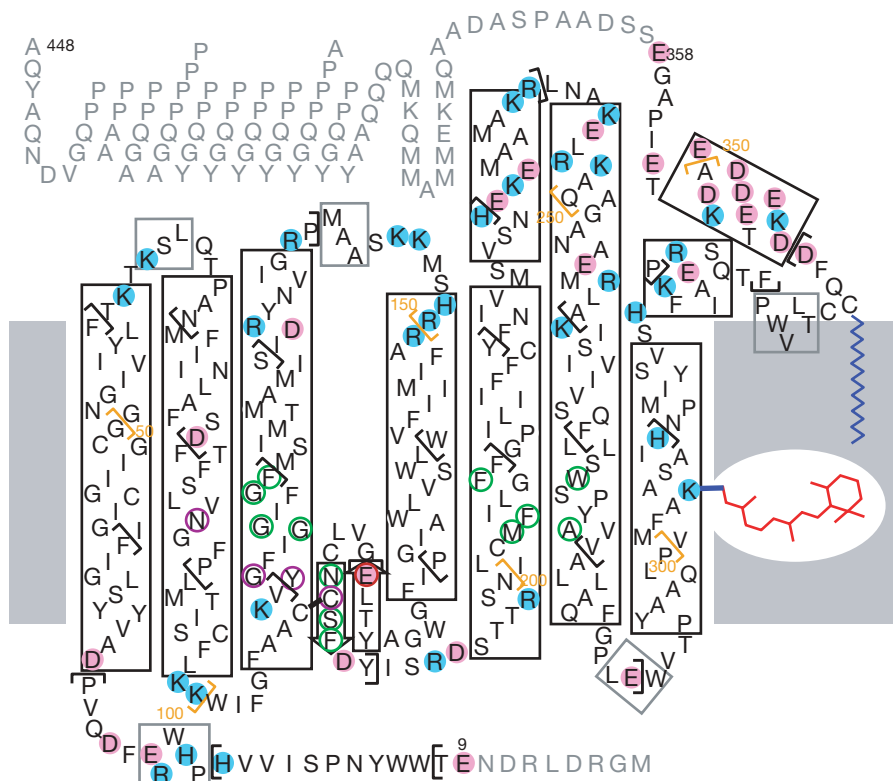


**Figure 1 | Schematic diagram of the topology of squid rhodopsin.**  $\alpha$ -Helices are denoted by black rectangles,  $3_{10}$  helices as grey rectangles and  $\beta$ -strands as open arrows. In the current structural model, the polypeptide chain is traced from Glu 9 to Glu 358 (shown by black letters). Grey letters indicate residues that are truncated or disordered. Retinal bound to Lys 305 and palmitoyl bound to Cys 337 are included in the structural model. A disulphide bond is formed between Cys 108 and Cys 186. The counterion Glu 180, residues within 3.5 Å of the Schiff base and within 4 Å of the retinal polyene chain are circled by red, purple and green lines, respectively. Positively and negatively ionizable residues are marked with blue and pink circles, respectively.

<sup>1</sup>Department of Physics, Graduate School of Science, Nagoya University, Nagoya 464-8602, Japan. <sup>2</sup>RIKEN Harima Institute/SPRING-8, 1-1-1, Kouto, Sayo, Hyogo 679-5148, Japan.

deletion does not affect the ability of rhodopsin to activate G proteins<sup>8</sup>. In this study, the C-terminal extension was removed by cleaving a peptide bond at Glu 373 (or Glu 358) with V8-protease, and C-terminally truncated rhodopsin was crystallized according to a procedure described previously<sup>9,10</sup>. Briefly, the truncated rhodopsin was extracted selectively from the microvillar membranes with octylglucoside in the presence of zinc acetate and it was crystallized into the hexagonal  $P6_2$  crystal.

In this crystal form, the asymmetric unit contains two molecules with similar structures. In Fig. 2a, two adjacent subunits that are related by a local two-fold axis lying in the  $ab$  plane are drawn in red and blue. The N-terminal peptides of these subunits are associated tightly with each other by salt bridges between Arg 24 and Glu 25 of both subunits (Fig. 2c). It is feasible that the same type of protein–protein contact exists between adjacent microvillar membranes, contributing to the membrane organization into the hexagonally packed cylinders that are observed in the photoreceptor rhabdom<sup>11</sup>. In the crystal, another type of protein association is seen between two adjacent B-subunits that are related by a crystallographic two-fold axis (Fig. 2e). In this dimeric association, the

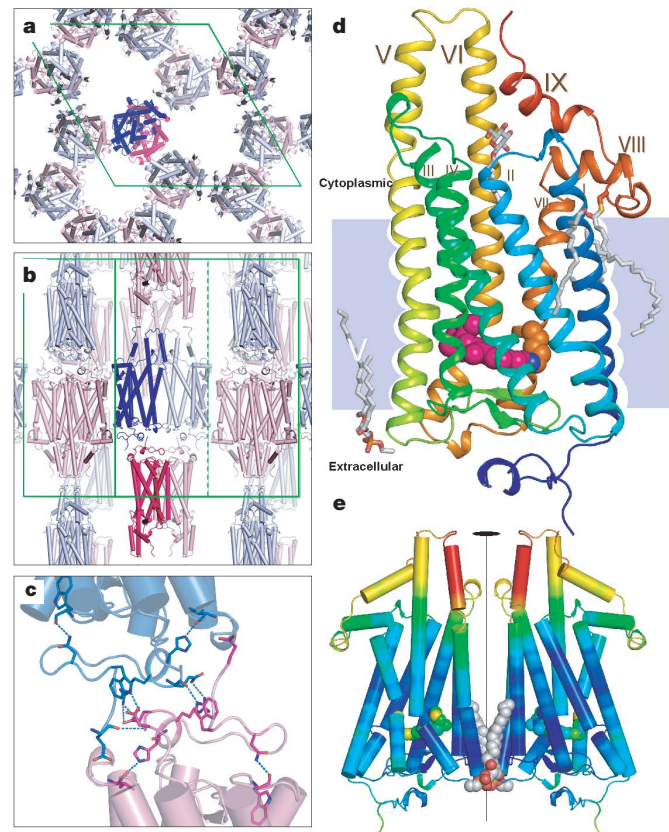


**Figure 2 | Crystal structure of C-terminally truncated squid rhodopsin.** **a, b,** Crystal packing viewed along the  $c$ -axis and  $a^*$ -axis, respectively. The subunits drawn in blue (A-subunit) and magenta (B-subunit) form a dimeric structure in the asymmetric unit. Such dimers are aligned around the  $c$ -axis as if they form a helical tube with double strands, in which interdimer contacts are formed between transmembrane helices I and II of A- and B-subunits with anti-parallel orientations. **c,** The dimer interface was maintained by salt bridges between Arg 24 and Glu 25 of both monomers. **d,** Side view of the B-subunit. Helices are colour-coded from blue (helix I) to red (helix IX). Retinal (magenta spacefill) is bound to Lys 305 via a protonated Schiff base (its nitrogen atom in blue). Cys 337 is palmitoyled (grey stick representation). One phospholipid and a fatty acid in interprotein space are shown in stick representation (grey). **e,** Side view of two adjacent B-subunits related by a crystallographic two-fold axis (vertical line). Helices are drawn in cylinder representation and colour-coded according to the B-factor of C $\alpha$  atom, from blue (lowest B factor: 33 Å<sup>2</sup>) to red (highest B factor: 118 Å<sup>2</sup>). All images were drawn with Pymol<sup>32</sup>.

protein–protein interactions are reinforced by phospholipids bound to intradimer crevices. This dimeric structure is similar in geometry to a dimer model that was recently proposed to explain atomic force micrographs of rat disc membranes<sup>12</sup>. However, as two adjacent A-subunits are differently arranged around the crystallographic two-fold axis, it is possible that the protein association within the same membrane is weaker than the intermembrane protein–protein association.

### Overall structure

C-terminally truncated rhodopsin, the polypeptide of which is traced from Glu 9 to Glu 358, is composed of seven transmembrane helices (from I to VII) and two cytoplasmic helices (VIII and IX) (Fig. 2d). Notably, helices V and VI protrude into the cytoplasmic medium, forming a column projecting 25 Å from the membrane surface. The presence of this column has been implicated by a low-resolution electron-density map of squid rhodopsin in a two-dimensional crystal<sup>13</sup>. Helix V is divided into a membrane-embedded region and a medium-exposed region; owing to a flexible joint at Ser 226, the latter helical part has a large motional freedom (Fig. 2e). In contrast, helix VI extends into the medium as a rigid spiral and its hydrophilic extension interacts with the C-terminal end of helix IX. Although helix IX contains many acidic residues, its motional freedom is suppressed by interactions with helix VIII, which is anchored to the cytoplasmic membrane surface by a palmitoyl group attached to Cys 337. Such an organized protein folding in the cytoplasmic

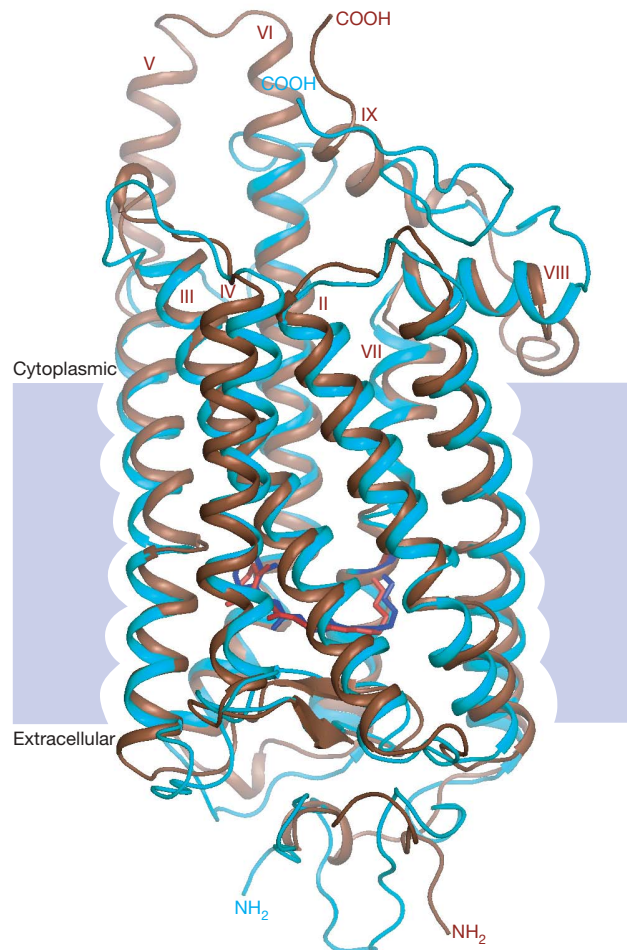


**Figure 3 | Structural comparisons between squid rhodopsin and bovine rhodopsin.** Squid rhodopsin is denoted by brown and magenta; bovine rhodopsin by cyan and blue.

medium is invisible in bovine rhodopsin<sup>14–16</sup>. The unique architecture of the cytoplasmic domain of squid rhodopsin provides an important insight into the recognition mechanism of a particular type of G protein.

In Fig. 3, the structure of squid rhodopsin is compared with that of bovine rhodopsin in a tetragonal  $P4_1$  crystal<sup>15</sup>. The most notable difference is seen in the third cytoplasmic (C3) loop. This difference is attributable to the extra sequence that squid rhodopsin possesses in this loop region. The multiple sequence alignment of squid and bovine rhodopsins is shown in Supplementary Fig. 1. As the C3 loop of bovine rhodopsin takes a different conformation in a different crystal form<sup>16</sup>, it has been argued that under physiological conditions the G-protein-binding site in the dark state of bovine rhodopsin is dynamically disordered. A flexible conformation of the C3 loop has been suggested previously in the  $\beta_2$ -adrenergic receptor<sup>17,18</sup>, which is another GPCR with known structure. Conversely, in squid rhodopsin the hydrophilic extension of helix VI takes a rigid conformation. As the amino acid sequence in this region is well conserved among invertebrate rhodopsins and other  $G_q$ -coupled receptors<sup>19</sup>, the extension of helices V and VI into the cytoplasmic medium can be regarded as an important structural motif for specifying the coupling mode with  $G_q$ -type G proteins.

Another unique feature of squid rhodopsin is a short  $3_{10}$  helix formed in an interhelical loop between helices VIII and IX. This  $3_{10}$  helix is dipped in the hydrophobic membrane region, whereas helix VIII is adhered to the hydrophilic surface of the lipid bilayer. Short  $3_{10}$  helices are also found in the N-terminal polypeptide and the third extracellular (E3) loop. These and other loops exposed to the extracellular medium are characterized by low temperature factors (Fig. 2e). The N-terminal polypeptide folds so as to interact with all of the extracellular loops. It may function as a scaffold for the folding of seven transmembrane helices, as proposed previously<sup>20</sup>.

### Structure of the retinal-binding pocket

As found in most GPCRs, squid rhodopsin possesses a disulphide bond between Cys 186 in the second extracellular (E2) loop and Cys 108 in helix III (Fig. 4a). This bond is important in the proper folding of the E2 loop into the membrane region, where it forms a  $\beta$ -sheet structure that functions as a plug of the retinal-binding pocket. The 11-*cis* retinal is bound covalently to Lys 305 on helix VII. The retinal–lysine chain takes a U-shaped configuration around the indole ring of Trp 274 on helix VI. The polyene chain is orientated perpendicularly to the membrane normal, whereas the  $\beta$ -ionone ring

is rotated by  $\sim 90^\circ$  with reference to the plane of the polyene chain. Five aromatic residues (Phe 120, Phe 188, Phe 205, Phe 209 and Trp 274) are positioned around the  $\beta$ -ionone ring, and together with Met 204, they form a rigid hydrophobic pocket. The central part (C9 to C14 atoms) of retinal is sandwiched by the main chain of helix III (Gly 112, Gly 115, Gly 116 and Gly 119) and a  $\beta$ -strand (Cys 186, Ser 187 and Phe 188) in the E2 loop; its cytoplasmic side is capped by Trp 274. The present results show that residues in contact with retinal are largely altered from those seen in bovine rhodopsin. Reflecting this alteration, the retinal polyene chain takes a less distorted configuration in squid rhodopsin than in bovine rhodopsin.

The anionic residue Glu 180, which is highly conserved among visual pigments, is too far from the retinyliden-bound nitrogen to have a direct interaction (Supplementary Table 2), and the side chain of Asn 185 is located between them. It is possible that after the photoisomerization of retinal, Asn 185 moves to mediate an indirect interaction between Glu 180 and the retinal Schiff base. The hydrogen-bonding partner of the Schiff base in the dark state is either the side-chain carbonyl of Asn 87 or the OH group of Tyr 111. These residues are conserved among invertebrate rhodopsins but are replaced by glycine (Gly 89) and glutamate (Glu 113), respectively, in bovine rhodopsin. A previous spectroscopic study of octopus rhodopsin has shown that the counterpart of Tyr 111 is kept neutral in both the dark state and the acid metarhodopsin state<sup>21</sup>. This implies that in invertebrate rhodopsins, Glu 180 is the sole anionic residue existing near the Schiff base.

### Water cluster in an interhelical cavity

Squid rhodopsin possesses a large interhelical cavity that is filled by nine water molecules. Together with two hydrophilic residues (Asp 80 and Asn 311) existing in the middle of this cavity, these water molecules form a long hydrogen-bonding network which extends from the retinal-binding pocket to a crevice of the cytoplasmic surface (Fig. 4b). In the innermost region of this network, water molecules interact with the main-chain carbonyls of Lys 305 and Ala 304 and the indole nitrogen atom of Trp 274. The other end of the network is terminated by the phenol group of Tyr 315 in the 'NPxxY' motif which is highly conserved in GPCRs. It is noteworthy that the number of water molecules existing in the interhelical cavity is much larger than that observed in bovine rhodopsin<sup>14,15</sup>. Squid rhodopsin can therefore be classified as a typical example of an 'inside-out protein'. This classification is useful for the better understanding of the photoactivation mechanism of squid rhodopsin. A recent Fourier

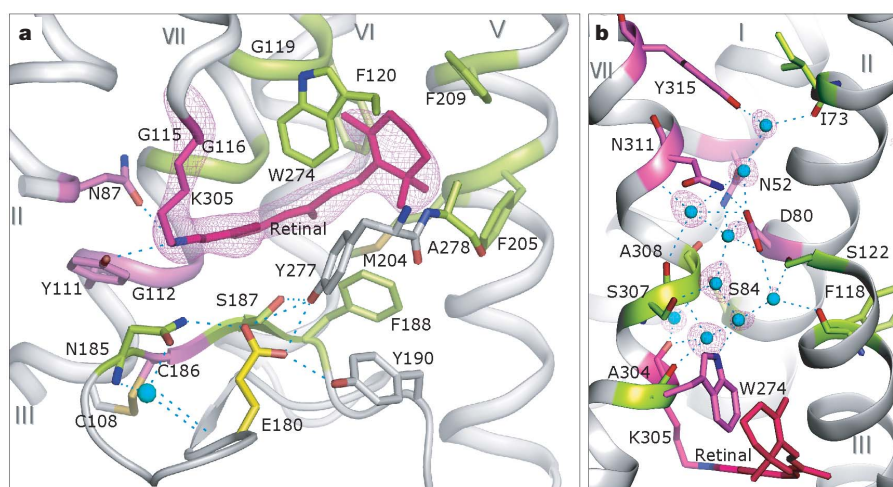


**Figure 4 | Retinal-binding pocket and interhelical cavity. a**, Structure of the retinal-binding pocket, with an omit map of the retinal Lys 305 chain contoured at  $5\sigma$  (purple mesh). Residues within 4 Å of the retinal polyene chain are drawn in green; residues in the vicinity of the Schiff base nitrogen atom are drawn in violet. Oxygen, nitrogen and sulphur atoms are in red,

blue and gold, respectively. **b**, Interhelical cavity filled by nine water molecules (cyan), with an omit map of the water molecules contoured at  $3.8\sigma$  (purple mesh). Residues that are well conserved among GPCRs are drawn in violet. For derivation of the omit maps, diffraction intensities from a partially twinned crystal were detwinned using Detwin in CCP4<sup>33</sup>.

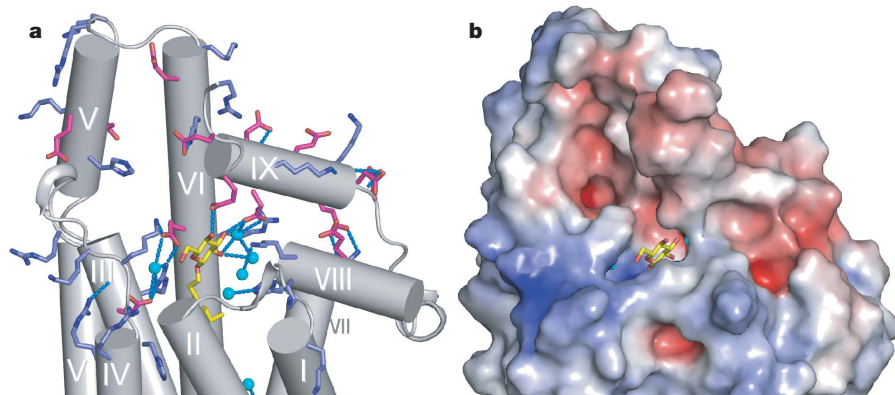


**Figure 5 | Cytoplasmic view of C-terminally truncated squid rhodopsin.** **a**, Octylglucoside bound to a crevice in the cytoplasmic protein surface is shown in yellow. Positively and negatively charged residues are drawn in

light blue and red, respectively. **b**, Electrostatic potential (red, negative; blue, positive) on the protein surface, viewed from the same direction as in **a**, is calculated with APBS<sup>34</sup>.

transform infrared spectroscopy study has shown that more than eight water molecules change their vibration frequencies on formation of bathorhodopsin<sup>22</sup>. It is thus suggested that a light-induced conformational change propagates towards the cytoplasmic side along the water cluster. It is conceivable that rearrangement of the water molecules inside the protein evokes a significant change in the local environment of functionally important residues such as Asp 80 and Asn 311. As these residues and their surrounding residues (Asn 52, Leu 76, Ala 77, Pro 312 and Tyr 315) are highly conserved among GPCRs, it is possible that the conformational change in the interhelical water cluster is crucial for the activation of G proteins.

### Insights into the photoactivation mechanism

The activation mechanism of transducin,  $G_t$ -type G protein, in vertebrate photoreceptors has been extensively studied. According to a recently proposed two-state interaction model<sup>23</sup>, the GDP/GTP exchange reaction in  $G_t$  proceeds as follows: (1) the state called metarhodopsin Ib binds GDP-bound  $G_t$ ; (2) the formation of metarhodopsin II is accompanied by a large structural change in the rhodopsin- $G_t$  complex; (3) GDP is released from the complex; and (4) GTP binds to the nucleotide-free  $G_t$ . It remains unclear whether the same reaction scheme is applicable to  $G_q$ -type G proteins. The crystal structure of squid rhodopsin shows that the carboxyl group of Asp 80 interacts directly with the side chain of Asn 311. As the linkage between their equivalent residues in GPCR has been reported to be coupled with the activation of G proteins<sup>24</sup>, it is possible that the crystal structure shown here corresponds to a state in which rhodopsin is able to bind G proteins. However, as the retinal in the crystal takes an 11-*cis* configuration, an alternative explanation is that squid rhodopsin in the dark state already has the ability to form a complex with GDP-bound  $G_q$ .

In this context, it is observed that the detergent octylglucoside is bound to a crevice in the cytoplasmic surface (Fig. 5a). This crevice is surrounded by helices II, III, IV and VII and is separated by a few hydrophobic residues from the interhelical water cluster. The tail moiety of octylglucoside interacts with the hydrophobic wall of the crevice, whereas its head group interacts with several polar residues which include: Asp 132 and Arg 133 in the 'DRY' motif; Ser 64 in helix I; Lys 321 in helix VIII; and Asp 347 and Glu 351 in helix IX. Octylglucoside binding seems to stabilize the conformation of the cytoplasmic domain, as described above. It is possible that octylglucoside mimics the C-terminal polypeptide of  $G\alpha_q$ , the 11 terminal residues of which are relevant to the selective recognition of a special type of GPCR<sup>25</sup>. It is notable that negatively and positively charged residues are distributed asymmetrically around a postulated binding site of the C-terminal polypeptide of  $G\alpha_q$ . The calculated map of electrostatic potential on the protein surface shows that positively

charged residues (Lys 145, Lys 146, Arg 150 and Arg 151) are crowded into the N-terminal end of helix IV and the C2 loop, whereas negatively charged residues are clustered along helix IX (Fig. 5b). Such charge distribution would have a significant effect on the binding mode of the G protein. It may also affect rhodopsin dimerization, which has been shown recently to be coupled with the activation process of G proteins<sup>12</sup>.

### Detection of the polarization plane

It has long been recognized that the invertebrate eye detects the polarization plane of visible light<sup>26,27</sup>. The crystal structure (Fig. 2) shows that two intermembrane dimers, around a crystallographic two-fold axis, form a tetrameric structure in which four retinylidene chromophores are orientated nearly parallel with one another. Under physiological conditions this tetramer may be characterized by a higher symmetry. It is possible that such tetramers are arranged in the apposed microvillar membranes so that the absorption dipole moments of all the retinal chromophores are aligned in parallel with the microvillar axis. As the microvillar membranes in each photoreceptor cell are orientated in a particular direction<sup>28</sup>, our crystal data provide an insight into the detection mechanism of the polarization plane.

Unlike vertebrate rhodopsin, the retinal chromophore in squid rhodopsin remains bound to the protein moiety under prolonged illumination. Its acid metarhodopsin state is thermally stable and, on absorption of visible light, it is hit back into the initial dark state<sup>29</sup>. At a moderate light intensity, the photoreactions of squid rhodopsin can be described by a two-photon cycle whose turnover rate is proportional approximately to  $\cos^4\alpha$ , where  $\alpha$  is the angle that is made by the absorption dipole moment of retinal and the polarization plane of incident light. This implies that a very sensitive detection system of the polarization plane would be acquired if the two-photon cycle is involved in the activation of G protein. Further investigation into the structure–function relationship of squid rhodopsin is needed to address questions such as which type of physical quantity (light intensity, colour or polarization) does the squid eye use to perceive objects, and how do G proteins interact with the dark state of squid rhodopsin. The latter is also crucial for elucidation of the activation mechanism of human melanopsin<sup>30</sup> and other  $G_q$ -type GPCRs.

### METHODS SUMMARY

Microvillar membranes from the photoreceptor rhabdoms in squid retina were purified using the sucrose flotation method. The purified microvillar membranes were treated with the enzyme V8-protease at 277 K for 12 h to cleave a specific site in the C-terminal extension of rhodopsin. C-terminally truncated rhodopsin was extracted selectively with octylglucoside in the presence of 30 mM zinc acetate. The final concentration of rhodopsin was  $\sim 10 \text{ mg ml}^{-1}$ . Crystals of the truncated rhodopsin were grown at 277 K by the sitting-drop

vapour-diffusion method, from a mixture solution containing ammonium sulphate and EDTA, pH 6.4. A single crystal was cryoprotected in 20% sucrose and was flash-frozen with liquid propane. X-ray diffraction measurements were performed at SPring8-BL38B1, where a frozen crystal kept at 100 K was exposed to a monochromatic X-ray beam at a wavelength of 1.0 Å with an X-ray flux rate of  $4 \times 10^{12}$  photons  $\text{mm}^{-2} \text{s}^{-1}$ .

Although the total X-ray dose per one data set ( $4 \times 10^{15}$  photons  $\text{mm}^{-2}$ ) exceeded a safety level that had been deduced from X-ray-induced absorption changes in bacteriorhodopsin crystals<sup>31</sup>, there was no detectable difference between the electron-density maps derived from two data sets taken sequentially. Therefore, no attempt was made to correct possible X-ray damage in the retinal configuration. The structure of squid rhodopsin was solved by molecular replacement, using a membrane-embedded part of bovine rhodopsin (Protein Data Bank accession 1gzmm) as an initial search model. Data collection and refinement statistics are shown in Supplementary Table 1.

**Full Methods** and any associated references are available in the online version of the paper at [www.nature.com/nature](http://www.nature.com/nature).

Received 8 January; accepted 18 March 2008.

- Oldham, W. M. & Hamm, H. E. Heterotrimeric G protein activation by G-protein-coupled receptors. *Nature Rev. Mol. Cell Biol.* **9**, 60–71 (2008).
- Hubbard, R. & St George, R. C. The rhodopsin system of the squid. *J. Gen. Physiol.* **41**, 501–528 (1958).
- Yarfitz, S. & Hurley, J. B. Transduction mechanisms of vertebrate and invertebrate photoreceptors. *J. Biol. Chem.* **269**, 14329–14332 (1994).
- Shichida, Y. & Imai, H. Visual pigment: G-protein-coupled receptor for light signals. *Cell. Mol. Life Sci.* **54**, 1299–1315 (1998).
- Terakita, A., Yamashita, T., Tachibanaki, S. & Shichida, Y. Selective activation of G-protein subtypes by vertebrate and invertebrate rhodopsins. *FEBS Lett.* **439**, 110–114 (1998).
- Hara-Nishimura, I. *et al.* Cloning and nucleotide sequence of cDNA for rhodopsin of the squid *Todarodes pacificus*. *FEBS Lett.* **317**, 5–11 (1993).
- Williamson, M. P. The structure and function of proline-rich regions in proteins. *Biochem. J.* **297**, 249–260 (1994).
- Ashida, A., Matsumoto, K., Ebrey, T. G. & Tsuda, M. A purified agonist-activated G-protein coupled receptor: truncated octopus acid metarhodopsin. *Zoolog. Sci.* **21**, 245–250 (2004).
- Murakami, M., Kitahara, R., Gotoh, T. & Kouyama, T. Crystallization and crystal properties of squid rhodopsin. *Acta Crystallogr. F* **63**, 475–479 (2007).
- Venien-Bryan, C. *et al.* Effect of the C-terminal proline repeats on ordered packing of squid rhodopsin and its mobility in membranes. *FEBS Lett.* **359**, 45–49 (1995).
- Saibil, H. & Hewat, E. Ordered transmembrane and extracellular structure in squid photoreceptor microvilli. *J. Cell Biol.* **105**, 19–28 (1987).
- Liang, Y. *et al.* Organization of the G protein-coupled receptors rhodopsin and opsin in native membranes. *J. Biol. Chem.* **278**, 21655–21662 (2003).
- Davies, A. *et al.* Three-dimensional structure of an invertebrate rhodopsin and basis for ordered alignment in the photoreceptor membrane. *J. Mol. Biol.* **314**, 455–463 (2001).
- Palczewski, K. *et al.* Crystal structure of rhodopsin: A G protein-coupled receptor. *Science* **289**, 739–745 (2000).
- Okada, T. *et al.* The retinal conformation and its environment in rhodopsin in light of a new 2.2 Å crystal structure. *J. Mol. Biol.* **342**, 571–583 (2004).
- Li, J. *et al.* Structure of bovine rhodopsin in a trigonal crystal form. *J. Mol. Biol.* **343**, 1409–1438 (2004).
- Cherezov, V. *et al.* High-resolution crystal structure of an engineered human  $\beta_2$ -adrenergic G protein-coupled receptor. *Science* **318**, 1258–1265 (2007).
- Rasmussen, S. G. F. *et al.* Crystal structure of the human  $\beta_2$  adrenergic G-protein-coupled receptor. *Nature* **450**, 383–387 (2007).
- Horn, F. *et al.* GPCRDB: an information system for G protein-coupled receptors. *Nucleic Acids Res.* **26**, 275–279 (1998).
- Doi, T., Molday, R. S. & Khorana, H. G. Role of the intradiscal domain in rhodopsin assembly and function. *Proc. Natl Acad. Sci. USA* **87**, 4991–4995 (1990).
- Nakagawa, M. *et al.* How vertebrate and invertebrate visual pigments differ in their mechanism of photoactivation. *Proc. Natl Acad. Sci. USA* **96**, 6189–6192 (1999).
- Ota, T. *et al.* Structural changes in the Schiff base region of squid rhodopsin upon photoisomerization studied by low-temperature FTIR spectroscopy. *Biochemistry* **45**, 2845–2851 (2006).
- Morizumi, T., Imai, H. & Shichida, Y. Y. Direct observation of the complex formation of GDP-bound transducin with the rhodopsin intermediate having a visible absorption maximum in rod outer segment membranes. *Biochemistry* **44**, 9936–9943 (2005).
- Urizar, E. *et al.* An activation switch in the rhodopsin family of G protein-coupled receptors. *J. Biol. Chem.* **280**, 17135–17141 (2005).
- Hamm, H. E. *et al.* Site of G protein binding to rhodopsin mapped with synthetic peptides from the alpha subunit. *Science* **241**, 832–835 (1988).
- Jander, P., Daumer, K. & Waterman, T. H. Polarized light orientation by two hawaiian decapod cephalopods. *J. Comp. Physiol. A* **46**, 383–394 (1963).
- Saidel, W. M., Shashar, N., Schmolesky, M. T. & Hanlon, R. T. Discriminative responses of squid (*Loligo pealeii*) photoreceptors to polarized light. *Comp. Biochem. Physiol. A* **142**, 340–346 (2005).
- Saibil, H. R. An ordered membrane-cytoskeleton network in squid photoreceptor microvilli. *J. Mol. Biol.* **158**, 435–456 (1982).
- Naito, T., Nashima-Hayama, K., Ohtsu, K. & Kito, Y. Photoreactions of cephalopod rhodopsin. *Vision Res.* **21**, 935–941 (1981).
- Provencio, I. *et al.* Melanopsin: An opsin in melanophores, brain, and eye. *Proc. Natl Acad. Sci. USA* **95**, 340–345 (1998).
- Matsui, Y. *et al.* Specific damage induced by X-ray radiation and structural changes in the primary photoreaction of bacteriorhodopsin. *J. Mol. Biol.* **324**, 469–481 (2002).
- DeLano, W. L. The PyMOL Molecular Graphics System. (<http://www.pymol.org>) (2002).
- Bailey, S. The CCP4 suite: programs for protein crystallography. *Acta Crystallogr. D* **50**, 760–763 (1994).
- Baker, N. A. *et al.* Electrostatics of nanosystems: Application to microtubules and the ribosome. *Proc. Natl Acad. Sci. USA* **98**, 10037–10041 (2001).

**Supplementary Information** is linked to the online version of the paper at [www.nature.com/nature](http://www.nature.com/nature).

**Acknowledgements** This work was supported by Grant-in-Aids from the Ministry of Education, Science and Culture of Japan and partly by the National Project on Protein Structural and Functional Analyses.

**Author Contributions** T.K. and M.M. designed the project. M.M. performed all experiments. T.K. assisted in data collection and structure determination. T.K. and M.M. jointly wrote the manuscript.

**Author Information** The coordinates have been deposited in the Protein Data Bank under accession number 2z73. Reprints and permissions information is available at [www.nature.com/reprints](http://www.nature.com/reprints). Correspondence and requests for materials should be addressed to T.K. ([kouyama@bio.phys.nagoya-u.ac.jp](mailto:kouyama@bio.phys.nagoya-u.ac.jp)).

## METHODS

**Materials.** Fresh squid (*Todarodes pacificus*) were purchased from Yanagibashi fish market in Nagoya, Japan. All chemicals were obtained from Wako Pure Chemical Industries with the exception of the endoprotease Glu-C from *Staphylococcus aureus* V8 (V8-protease), which was purchased from Sigma-Aldrich.

**Membrane purification.** All manipulations were performed under dim red light (>640 nm) at 277 K unless otherwise stated. Microvillar membranes from rhabdomeric photoreceptor cells of squid retina were purified according to the method described previously<sup>35</sup>. Briefly, crude microvillar membranes were isolated in phosphate buffer (50 mM NaPO<sub>4</sub>, pH 6.8, 4% NaCl, 1 mM EDTA, 0.1 mM phenylmethylsulfonyl fluoride, 1 mM dithiothreitol; 0.2 μg ml<sup>-1</sup> leupeptin, 0.01% NaN<sub>3</sub>) using the sucrose flotation method. After sucrose step-gradient centrifugation of the microvillar membranes, rhodopsin-rich membranes were collected from the interface between the 20% and 32% (w/v) sucrose layers and washed with water at least three times to remove peripheral components.

**Truncation of the C-terminal extension of rhodopsin.** The purified microvillar membranes (~5 mg ml<sup>-1</sup> rhodopsin) were treated with the enzyme V8-protease (100:1 (w/w) rhodopsin:enzyme) at 277 K over 12 h to cleave at a specific site in the C-terminal extension of rhodopsin. The reaction was terminated by repeated washing of the microvillar membranes. The washed microvillar membranes were suspended in a minimum volume of water and the rhodopsin concentration was determined from the absorbance at 480 nm using the reported absorption coefficient of 35,000 mol<sup>-1</sup> cm<sup>-1</sup> (ref. 36). The membrane suspension containing ~10 mg ml<sup>-1</sup> C-terminally truncated rhodopsin was stored at 193 K until further purification.

**Selective extraction of rhodopsin.** Selective extraction of C-terminally truncated rhodopsin from the microvillar membranes was performed according to the method developed for purification of bovine rhodopsin<sup>37</sup> with minor modifications. C-terminally truncated squid rhodopsin was extracted selectively from the microvillar membranes by mixing the membrane suspension with a buffer/detergent solution giving the final concentrations: 30 mM MES, pH 6.4, 30 mM zinc acetate, and ~100 mM octylglucoside with a detergent/protein ratio of ~3.7 (w/w). After incubation at 277 K overnight, the mixture was centrifuged at 30,000 r.p.m. for 1 h and the supernatant was used within one day for crystallization.

**Crystallization.** The extracted rhodopsin was crystallized at 277 K by the sitting-drop vapour-diffusion method using commercially available crystallization kits (Vapour Diffusion Crystalplate, ICN Biomedicals). The protein solution was mixed with an equal volume of a reservoir solution containing 3.2 M ammonium sulphate, 32 mM MES pH 6.4, 38 mM EDTA and 10 mM β-mercaptoethanol. A drop (10 μl) of the mixture was equilibrated against 0.5 ml of the reservoir solution. After incubation at 277 K for >six months, hexagonal crystals had grown in size to 200 μm.

**Data collection.** A single crystal was transferred into a solution containing 30 mM octylglucoside, 3.2 M ammonium sulphate, 40 mM MES pH 6.4 and 20% sucrose. After soaking for 10 min, the crystal was flash-frozen in liquid propane held at its melting temperature and was stored in liquid nitrogen. X-ray diffraction measurements were performed at SPring8-BL38B1, where a frozen crystal kept at 100 K was exposed to a monochromatic X-ray beam at a wavelength of 1.0 Å with an X-ray flux rate of 4 × 10<sup>12</sup> photons mm<sup>-2</sup> s<sup>-1</sup>. Indexing and integration of diffraction spots were carried out with Mosflm 6.2 (ref. 38). The scaling of data was carried out using SCALA in the CCP4 program suites<sup>33</sup>. Data statistics are shown in Supplementary Table 1.

**Structure refinement.** Structure refinement was done with CNS-1.1<sup>39</sup> and XtalView-4.0<sup>40</sup>. Diffraction data from the hexagonal crystal were fitted well by unit-cell parameters  $a = b = 122.6 \text{ \AA}$ ,  $c = 158.7 \text{ \AA}$ ,  $\alpha = \beta = 90^\circ$ , and  $\gamma = 120^\circ$ . Inspection of diffraction spots along the *c*-axis indicated the presence of a crystallographic three-fold screw axis. After various trials, the space group was assigned to *P*6<sub>2</sub>. The model building was performed by the molecular-replacement method with a membrane-embedded part of bovine rhodopsin (Protein Data Bank accession 1GZM) as an initial search model. Diffraction intensities from a partially twinned crystal (twinning fraction ~0.24) were detwinned by CCP4 and the resultant intensities  $I_{\text{detwin}}(hkl)$  were used to build a structural model at 2.6 Å resolution. This model was further refined with a higher resolution data set from a nearly perfect twin. In this case, diffraction intensities were detwinned by the equation:

$$I_{\text{detwin}}(hkl) = \{2 \langle I_{\text{obs}}(hkl) \rangle + I_{\text{calc}}(hkl) - I_{\text{calc}}(k, h, -l)\} / 2$$

where  $\langle I_{\text{obs}}(hkl) \rangle = (I_{\text{obs}}(hkl) + I_{\text{obs}}(k, h, -l)) / 2$  and  $I_{\text{calc}}$  is the intensity calculated from the model.

35. Kito, Y., Naito, T. & Nashima, K. Purification of squid and octopus rhodopsin. *Methods Enzymol.* **81**, 167–171 (1982).
36. Suzuki, T., Uji, K. & Kito, Y. Studies on cephalopod rhodopsin: photoisomerization of the chromophore. *Biochim. Biophys. Acta* **428**, 321–338 (1976).
37. Okada, T., Takeda, K. & Kouyama, T. Highly selective separation of rhodopsin from bovine rod outer segment membranes using combination of divalent cation and alkyl (thio) glucoside. *Photochem. Photobiol.* **67**, 495–499 (1998).
38. Steller, I., Bolotovskiy, R. & Rossmann, M. G. An algorithm for automatic indexing of oscillation images using Fourier analysis. *J. Appl. Crystallogr.* **30**, 1036–1040 (1997).
39. Brunger, A. T. *et al.* Crystallography & NMR system: A new software suite for macromolecular structure determination. *Acta Crystallogr. D* **54**, 905–921 (1998).
40. McRee, D. E. *Practical Protein Crystallography* (Academic, San Diego, 1993).